Original Research Article

Solar Radiation Energy Issues on Nanoparticle Shapes in the Potentiality of Water-based Cu, Al₂O₃ and SWCNTs

Ramasamy Kandasamy*, Nur Atikahbt Adnan, Mohd Kamarulzaki, Mohd Saifullah

Faculty of Applied Science and Technology, Universiti Tun Hussein Onn Malaysia, Pagoh, Johor, 84600Malaysia.

*Correspondence: ramasamy@uthm.edu.my

ABSTRACT

Energy is an extensive view for industrial advancement. Solar thermal energy is designed by light and heat which is radiated by the sun, in the form of electromagnetic radiation. Solar energy is the highest promptly and sufficiently applicable authority of green energy. Impact of nanoparticle shapes on the Hiemenz nanofluid (water-based Cu, Al2O3 and SWCNTs) flow over a porous wedge surface in view of solar radiation energy has been analyzed. The three classical form of nanoparticle shapes are registered into report, i.e. sphere (m=3.0), cylinder (m=6.3698) and laminar (m=16.1576). Nanoparticles in the water-based Cu, Al₂O₃ and SWCNTs have been advanced as a means to boost solar collector energy through explicit absorption of the entering solar energy. The controlling partial differential equations (PDEs) are remodeled into ordinary differential equations (ODEs) by applying dependable accordance alteration and it is determined numerically by executing Runge Kutta Fehlberg method with shooting technique. It is anticipated that the lamina shape SWCNTs have dynamic heat transfer attainments in the flow improvement over a porous wedge surface as compared with the other nanoparticle shapes in different nanofluid flow regime.

Keywords: Nanoparticle Shapes; Unsteady Hiemenz Flow; Water-based Cu, Al₂O₃ and SWCNTs, Solar Energy Radiation

1. Introduction

Recently nanofluid (water-based Cu, Al₂O₃ and SWCNTs) attracts a noticeable application due to its remarkably energetic heat transfer mechanism. Solar thermal energy is an ideal significant in our regular benefit and it's a usual system of accessing heat, electricity and water with assist from the nature. As we will address some fossil fuels situation, the solar thermal energy is a sustainable expert of energy which never exhausts. Sustainable energy generation is one of the most important challenges facing society today. Solar thermal energy is one of the principal experts of renewable energy with basic coincidental impact, Sharma et al.[1]. The essential view of adopting particles to assemble solar energy was analyzed in the 1970s by Hunt[2]. Nanoparticles attempt the possible of developing the radiative assets of liquids, outstanding to enhance in the capability of explicit absorption solar collectors. Heat transfer in the nanofluids (water based Cu, Al₂O₃ and SWCNTs) due to solar radiation energy is of considerable practical influence to engineers and scientists as a result of its relatively global event in countless units of science and engineering, Choi[3], Buongiorno and Hu[4], Buongiorno[5] and Cheng and Minkowycz[6]. Once again, science and progressive technology are much obliged to solar radiation due to its extensive utilization in the design of solar thermal electricity, solar photovoltaic cells, solar heating, artificial photosynthesis, etc.

Nanoparticle shapes (sphere, cylinder and lamina) in the nanofluids (water-based Cu, Al₂O₃ and SWCNTs) absorb solar radiation notably because of small size as correlated to the wavelength of de Broglie wave. Therefore nanoparticles also attempt the assuring aspect of strengthening the radiative resources of liquids, dominating to accelerate in the performance of straight absorption of solar collectors[7,8]. Recently, the effects of solar radiation on nanofluid with variable stream conditions were addressed by Das et al.[9] and Anbuchezhian et al.[10].

Many investigators[11-15] have analyzed the utilization of these new transport of heat transfer in solar collectors. Yousefi et al.[11] experimentally presented that the Al$_2$O$_3$/water nanofluid increases the ability of flat-plate collectors by 28.3%. Yousefi et al.[12] studied the effects of pH values of carbon nanotube nanofluids on the expertise of a flat-plate solar collector. Kameya and Hanamura[13] addressed that the radiation absorption resources of base fluid were increased harmfully by including Ni nanoparticles. Lenert and Wang[14] analyzed the efficiency of nanofluids as volumetric receivers in concentrated solar utilizations applying the suspension of carbon-coated cobalt nanoparticles into Therminol VP-1 fluid. He et al.[15] practically addressed the applicable photo-thermal assets of Cu/H$_2$O nanofluids for enrollment in blunt absorption, solar thermal energy systems.

Furthermore, the up-to-date revision papers[17,18] recorded that nanofluids had strong accessible for utilizations in solar organizations such as solar collectors[19], photovoltaic thermal schemes[20], and thermal energy storage structures[21]. Most of the analysis on the employment of nanofluids in solar collectors have been defined to energy and exergy investigations. There are some analyses on the investigation of the hydrodynamic and convective heat transfer assets of nanofluids in solar structures[16]. As displayed in many review articles[22,23] and[24], a massive amount of practical work has been addressed on the thermal attitude of various types of nanofluids flowing through different heat exchanger models; among them, the circular successive tubes have admitted more application in this study since they are the main elemental of various types of solar collectors.

Recently, the capability of applying both nanofluid and porous media has admitted comfortable absorption and has attended to broad analysis in this field. Porous media enhance the association surface area among liquid and solid surface, and, on the other hand, nanoparticles circulated in nanofluid upgrade the impressive thermal conductivity. Therefore, it suggests that utilizing both porous media and nanofluid can enhance the ability of typical thermal systems harmfully. Convective flow in porous media has been universally analyzed in the recent years due to its extensive operations in engineering as post-accidental heat dismissal in solar heater or collectors, drying generating processes, heat exchangers system, geothermal and oil recovery scheme, building construction region, etc. Heat and mass transfer for Hiemenz flow through porous media in the presence of an incident external magnetic field have been studied by several authors[25-30].

The method of Lie group transformations is used to derive all group-invariant similarity solutions of the unsteady two-dimensional laminar boundary layer equations, Yurusoy and Pakdemirli[18], Yurusoy and Pakdemirli[19] and Avramenko et al.[37]. Impact of thermal stratification is an important aspect in heat transfer analyses. Thermal stratification of nanofluids occurs due to temperature variations or the presence of different fluids of different densities.

Figure 1: Flow configuration and coordinate system.

In this article, we addressed the role of nanoparticle shapes (sphere, cylinder and lamina) in the presence of unsteady nanofluids (water-based Cu, Al$_2$O$_3$ and SWCNTs) flow and heat transfer past a porous wedge sheet due to solar radiation. Lie symmetry group transformation is applied to transform the controlling PDEs into ODEs and then the numerical solution of the problem is cultivated by using fourth or fifth order Runge Kutta Fehlberg method with shooting technique. Experimental works have analyzed that the nanoparticle shape has a unique impact on the heat and mass transfer of nano-fluids[38,39]. Nanoparticle shapes i.e. sphere, cylinder and laminar, are authorized into address in this work. The parameter

affirmation for the problem was accomplished and is authorized. It is consumed that the results will gift towards better understanding of nanofluid conflict in channel. Several aspects of the problem are analyzed and predicted graphically with account to the physical parameters elaborated within it and the instant improvements are associated with the applicable literature.

2. Mathematical analysis

Consider the unsteady laminar two-dimensional flow of an incompressible viscous nanofluids (water-based Cu, Al_2O_3 and SWCNTs) past a porous wedge sheet in the presence of solar energy radiation (see, Figure 1). The porous medium is assumed to be transparent and in thermal equilibrium with the fluid and neglecting the pressure gradient in the y direction. Due to heating of the entrancing nanofluid and the wedge surface by solar thermal radiation, heat is transmitted from the plate. Also, the solar radiation is a collimated beam that is normal to the plate. The working water-based Cu, Al_2O_3 and SWCNTs nanofluid flow is assigned to be Newtonian. The system of regulating equations are designated:

$$\frac{\partial \bar{u}}{\partial \bar{x}} + \frac{\partial \bar{v}}{\partial \bar{y}} = 0 \qquad (1)$$

$$\frac{\partial \bar{u}}{\partial \bar{t}} + \bar{u}\frac{\partial \bar{u}}{\partial \bar{x}} + \bar{v}\frac{\partial \bar{u}}{\partial \bar{y}} = \frac{1}{\rho_{f_n}}[U\frac{dU}{dx}\rho_{f_n} + \mu_{f_n}\frac{\partial^2 \bar{u}}{\partial \bar{y}^2} + (\rho\beta)_{f_n}\bar{g}(T-T_\infty)\cos\frac{\Omega}{2} - \frac{v_f}{K}\rho_{f_n}(\bar{u}-U)] \quad (2)$$

$$\frac{\partial T}{\partial \bar{t}} + \bar{u}\frac{\partial T}{\partial \bar{x}} + \bar{v}\frac{\partial T}{\partial \bar{y}} = \alpha_{f_n}\frac{\partial^2 T}{\partial \bar{y}^2} - \frac{1}{(\rho c_p)_{f_n}}\frac{\partial q''_{rad}}{\partial y} \qquad (3)$$

Employing Rosseland approximation for thermal radiation (Sparrow and Cess[40], Rapits[41] and Brewster[42]),

$$q''_{rad} = -\frac{4\sigma_1}{3k^*}\frac{\partial T^4}{\partial y},$$

where σ_1 is the Stefan-Boltzman constant, k^* is the mean absorption coefficient. The Rosseland relation is recycled to define the thermal radiative heat transfer of the optically thick (nano-)fluid with boundary conditions.

$$\bar{u} = 0, \bar{v} = -v_0, T = T_w + c_1 x^{n_1} \ at \ \bar{y} = 0 \quad \bar{u} \to U = \frac{v\, x^m}{\delta^{m+1}}, T \to T_\infty = (1-n)T_o + nT_w \ as \ \bar{y} \to \infty \quad (4)$$

where c_1 and n_1 (power index) are constants; V_0 and T_w are the suction ($V_0 > 0$) or injection ($V_0 < 0$) velocity and the temperature at the plate. The feasible flow velocity of the wedge is:

$$U(x,t) = \frac{v\, x^m}{\delta^{m+1}}, \beta_1 = \frac{2m}{1+m} \quad (\text{Sattar}[43])$$

whereas δ is the time-dependent length scale, $\delta = \delta(t)$ and the Hartree pressure gradient parameter, $\beta_1 = \frac{\Omega}{\pi}$, Ω is the angle of the wedge, the temperature of the fluid is simulated to differ succeeding a power-law function while the free stream temperature is linearly stratified. In equation (4) and n is a constant parameter assigned as the thermal stratification parameter, $0 \le n < 1$, $T_0 = T_\infty(0)$ is a constant reference temperature. The suffixes w and ∞ denote surface and ambient conditions. $\bar{u}$ and $\bar{v}$ are the velocity components along the $\bar{x}$ and $\bar{y}$ directions. T is the local temperature of the nanofluid; $\bar{g}$ is the acceleration due to gravity; K is the permeability of the porous medium; ρ_{f_n} is the effective density of the nanofluid, q''_{rad} is the applied absorption radiation heat transfer; μ_{f_n} is the effective dynamic viscosity of the nanofluid, α_{f_n} is the thermal diffusivity of the nanofluid (Aminossadati Ghasemi[44]), which are defined as:

$$\rho_{f_n} = (1-\zeta)\rho_f + \zeta\rho_s \ , \ \mu_{f_n} = \frac{\mu_f}{(1-\zeta)^{2.5}} \ , \ (\rho\beta)_{f_n} = (1-\zeta)(\rho\beta)_f + \zeta(\rho\beta)_s \ , \ \alpha_{f_n} = \frac{k_{f_n}}{(\rho c_p)_{f_n}} \ ,$$

$$(\rho c_p)_{f_n} = (1-\zeta)(\rho c_p)_f + \zeta(\rho c_p)_s, \frac{k_{nf}}{k_f} = \left\{\frac{(k_s + (l-1)k_f) - (l-1)\zeta(k_f - k_s)}{(k_s + (l-1)k_f) + \zeta(k_f - k_s)}\right\} \qquad (5)$$

Maxwell model [45] was refined to define the effective electrical or thermal conductivity of liquid-solid suspensions. k_f and k_s are the thermal conductivity of the base fluid and nanoparticle, ζ is the nanoparticle volume fraction, μ_f is the the dynamic viscosity of the base fluid, β_f and β_s are the thermal expansion coefficients of the base fluid and nanoparticle, ρ_f and ρ_s are the density of the base fluid and nanoparticle, k_{f_n} is the effective thermal conductivity of the nanofluid and $(\rho c_p)_{f_n}$ is the heat capacitance of the nanofluid.

Proposing the succeeding non-dimensional variables:

$$x = \frac{\bar{x}}{\sqrt{\frac{v_f}{c}}}, y = \frac{\bar{y}}{\sqrt{\frac{v_f}{c}}}, u = \frac{\bar{u}}{\sqrt{c v_f}}, v = \frac{\bar{v}}{\sqrt{c v_f}} \text{ and } \theta = \frac{T - T_\infty}{T_w - T_\infty} \tag{6}$$

Based on the above results, the equations (1)-(4) become:

$$\frac{\partial u}{\partial x} + \frac{\partial v}{\partial y} = 0 \tag{7}$$

$$\frac{\partial u}{\partial t} + u \frac{\partial u}{\partial x} + v \frac{\partial u}{\partial y} = \frac{1}{(1 - \zeta + \zeta \frac{\rho_s}{\rho_f})}[\{\frac{\partial U}{\partial t} + U \frac{dU}{dx}\} \frac{\rho_{f_n}}{\rho_f} + \frac{v_f}{(1-\zeta)^{2.5}} \frac{\partial^2 u}{\partial y^2}$$
$$+ \{(1 - \zeta + \zeta \frac{(\rho \beta)_s}{(\rho \beta)_f}) \gamma \cos \frac{\Omega}{2} \theta\} - \frac{v_f}{K(1-\zeta)^{2.5}} (u - U)] \tag{8}$$

$$\frac{\partial T}{\partial t} + u \frac{\partial T}{\partial x} + v \frac{\partial T}{\partial y} = \frac{1}{1 - \zeta + \zeta \frac{(\rho c_p)_s}{(\rho c_p)_f}}[\frac{1}{Pr}\{\frac{k_{f_n}}{k_f} \frac{\partial^2 T}{\partial y^2} + \frac{4}{3} N((C_T + T)^3 \theta')\}] \tag{9}$$

with boundary conditions:

$$\bar{u} = 0, \bar{v} = -V_0, T = T_w \text{ at } \bar{y} = 0; \bar{u} \to U = \frac{v x^m}{\delta^{m+1}}, T \to T_\infty \to (1-n)T_o + nT_w \text{ as } \bar{y} \to \infty \tag{10}$$

$Pr = \frac{v_f}{\alpha_f}$ - the Prandtl number, $\lambda = \frac{\delta^{m+1}}{K k^2}$ - the porous media parameter, $\gamma = \frac{g (\rho \beta)_f \Delta T}{\rho_f U^2 k^{\frac{2}{1-m}}}$ - the buoyancy or natu-

ral convection parameter, $N = \frac{4 \sigma_1 \theta_w^3}{k_f k^*}$ - the conductive radiation parameter, where $\theta_w = \frac{1}{T_w - T_\infty} \cong 0.1$. Let $\gamma > 0$

aids the flow and $\gamma < 0$ opposes the flow, while $\gamma = 0$ i.e., $(T_w - T_\infty)$ represents the case of forced convection flow.

Hence, combined convective flow exists when $\gamma = O(1)$. Based on Kafoussias and Nanousis[20], $\eta = y \sqrt{\frac{(1+m)}{2}} \sqrt{\frac{x^{m-1}}{\delta^{m+1}}}$,

$$\psi = \sqrt{\frac{2}{1+m}} \frac{v x^{\frac{m+1}{2}}}{\delta^{\frac{m+1}{2}}} f(\eta) \text{ and } \theta = \frac{T - T_\infty}{T_w - T_\infty}, u = \frac{\partial \psi}{\partial y} \text{ and } v = -\frac{\partial \psi}{\partial x} \tag{11}$$

The system of equations (7)-(9) become:

$$\frac{\partial^2 \psi}{\partial t \partial y} + \frac{\partial \psi}{\partial y}\frac{\partial^2 \psi}{\partial x \partial y} - \frac{\partial \psi}{\partial x}\frac{\partial^2 \psi}{\partial y^2} = \frac{1}{(1-\zeta+\zeta\frac{\rho_s}{\rho_f})}[\{(1-\zeta+\zeta\frac{(\rho\beta)_s}{(\rho\beta)_f})\gamma\cos\frac{\Omega}{2}\theta\}$$

$$+\frac{1}{(1-\zeta)^{2.5}}\frac{\partial^3\psi}{\partial y^3} + \{\frac{\partial U}{\partial t}+U\frac{dU}{dx}\}\frac{\rho_{f_n}}{\rho_f} - \frac{v_f}{K(1-\zeta)^{2.5}}(\frac{\partial\psi}{\partial y}-U)] \tag{12}$$

$$\frac{\partial T}{\partial t} + \frac{\partial \psi}{\partial y}\frac{\partial T}{\partial x} - \frac{\partial \psi}{\partial x}\frac{\partial T}{\partial y} = \frac{1}{1-\zeta+\zeta\frac{(\rho c_p)_s}{(\rho c_p)_f}}[\frac{1}{Pr}\{\frac{k_{f_n}}{k_f}\frac{\partial^2\theta}{\partial y^2}+\frac{4}{3}N((C_T+T)^3\theta')'\}] \tag{13}$$

with the boundary conditions

$$\frac{\partial\psi}{\partial y}=0, \frac{\partial\psi}{\partial x}=-V_0, T=T_w \ at \ y=0; \frac{\partial\psi}{\partial y}\to\frac{v\,x^m}{\delta^{m+1}}, T\to T_\infty\to(1-n)T_o+nT_w \ as \ \bar{y}\to\infty \tag{14}$$

where $C_T = \frac{T_\infty}{T_W} - T_\infty$ is the temperature ratio, $C_T=0.1$ and heat radiation $0 \le N \le 1.0$, Murthy et al.

The symmetry groups of Equation (12) and (13) are estimated applying the classical Lie group approach as:

$$x^* = x + \varepsilon\xi_1(x,y,\psi,\theta), y^* = y + \varepsilon\xi_2(x,y,\psi,\theta),$$
$$\psi^* = \psi + \varepsilon\mu_1(x,y,\psi,\theta), \theta^* = \theta + \varepsilon\mu_2(x,y,\psi,\theta) \tag{15}$$

It is noted that the form of infinitesimals as:

$$\xi_1 = c_1 x + c_2, \xi_2 = g(x), \mu_1 = c_3\psi + c_4 \ and \ \mu_2 = c_5\theta$$

where *g(x)* is an arbitrary function. Definitions of the infinitesimal alternators are:

$$X_1 = x\frac{\partial}{\partial x} + g(x)\frac{\partial}{\partial y} + \psi\frac{\partial}{\partial\psi} + \theta\frac{\partial}{\partial\theta}, X_2 = \frac{\partial}{\partial x} + g(x)\frac{\partial}{\partial y}, X_3 = g(x)\frac{\partial}{\partial y} + \frac{\partial}{\partial\psi}$$

The PDEs controlling the work under attention are converted by a exclusive mode of Lie symmetry group conversions viz. one-parameter infinitesimal Lie group of transformation into a system of ODEs. For the current situation, we consider that the generator X_1 with *g(x)*=0. The distinctive equations are:

$$\frac{dx}{x} = \frac{dy}{0} = \frac{d\psi}{\psi} = \frac{d\theta}{\theta} \tag{18}$$

Based on the above equations, it is calculated as:

$$\eta = y, \psi = x\,f(\eta) \ and \ \theta = x\,\theta(\eta) \ where \ \eta = \eta(x,t) \tag{19}$$

Established on these relations, the Equations (12) and (13) become:

$$f''' - \frac{\frac{2}{m+1}(1-\zeta)^{2.5}\xi^2}{(1-\zeta+\zeta\frac{\rho_s}{\rho_f})}[\frac{\lambda}{(1-\zeta)^{2.5}}(f'-1)+\frac{m+1}{2}\lambda_v(2-2f'-\eta\,f'')-m-\xi^{\frac{1}{1-m}}\{(1-\zeta+\zeta\frac{(\rho c_p)_s}{(\rho c_p)_f})\}$$

$$\times\gamma\cos\frac{\Omega}{2}\theta]-(1-\zeta+\zeta\frac{\rho_s}{\rho_f})(1-\zeta)^{2.5}[\frac{2m}{m+1}f'^2-f\,f''+\frac{1-m}{1=m}\xi\frac{\partial f}{\partial\xi}(\frac{\partial f}{\partial\eta}-\frac{\partial^2 f}{\partial\eta^2})]=0 \tag{20}$$

$$\theta'' + \frac{4}{3}\frac{k_f}{k_{f_n}}N\{(C_T+\theta)^3\theta'\}' - Pr\{1-\zeta+\zeta\frac{(\rho c_p)_s}{(\rho c_p)_f}\}\frac{k_f}{k_{f_n}}$$

$$\times[\frac{2n_1}{m+1}\{\theta+\frac{n}{1-n}\}f'-f\theta'+\lambda_v\eta\,\theta'+\frac{1-m}{1+m}\{\xi\frac{\partial\theta}{\partial\xi}\frac{\partial f}{\partial\eta}-\xi\frac{\partial f}{\partial\xi}\frac{\partial\theta}{\partial\eta}\}]=0 \tag{21}$$

$$\frac{\partial f}{\partial \eta} = 0, \frac{m+1}{2} f + \frac{1-m}{2} \xi \frac{\partial f}{\partial \xi} = -S, \theta = 1 \text{ at } \eta = 0 \text{ and } \frac{\partial f}{\partial \eta} = 1, \theta \to 0 \text{ as } \eta \to \infty \tag{22}$$

S is the suction parameter if $S > 0$ and injection if $S < 0$. $\xi = kx^{\frac{1-m}{2}}$ is the dimensionless distance along the wedge ($\xi > 0$) (Kafoussias and Nanousis[50]). In this scheme of equations, it is predicted that the non-similarity forms of the problem are exhibited in the terms involving partial derivatives with respect to ξ. Generation of the local non-similarity schemes with reference to the current work will now be reviewed. At the first level of truncation, the terms followed by $\xi \frac{\partial}{\partial \xi}$ are small. This is notably true when ($\xi \ll 1$). Therefore the terms with $\xi \frac{\partial}{\partial \xi}$ on the right-hand sides of Equation (20) and (21) are eliminated to obtain the succeeding scheme of equations:

$$f''' - \frac{\frac{2}{m+1}(1-\zeta)^{2.5}\xi^2}{(1-\zeta+\zeta\frac{\rho_s}{\rho_f})} [\frac{\lambda}{(1-\zeta)^{2.5}}(f'-1) + \frac{m+1}{2}\lambda_v(2-2f'-\eta f'') - m$$
$$- \xi^{\frac{1}{1-m}}\{(1-\zeta+\zeta\frac{(\rho c_p)_s}{(\rho c_p)_f})\}\gamma \cos\frac{\Omega}{2}\theta] - (1-\zeta+\zeta\frac{\rho_s}{\rho_f})(1-\zeta)^{2.5}\{\frac{2m}{m+1}f'^2 - f f''\} = 0 \tag{23}$$

$$\theta'' + \frac{4}{3}\frac{k_f}{k_{f_n}}N\{(C_T+\theta)^3\theta'\}'$$
$$- \Pr\{1 - \zeta + \zeta\frac{(\rho c_p)_s}{(\rho c_p)_f}\}\frac{k_f}{k_{f_n}}[\frac{2n_1}{m+1}\{\theta + \frac{n}{1-n}\}f' - f\theta' + \lambda_v \eta \theta'] = 0 \tag{24}$$

with boundary conditions

$$f' = 0, f = -\frac{2S}{m+1}, \theta = 1 \text{ at } \eta = 0 \text{ and } f' = 1, \theta \to 0 \text{ as } \eta \to \infty \tag{25}$$

Suppose that $\lambda_v = \frac{c}{x^{m-1}}$, c is a constant so that $c = \frac{\delta^m}{v}\frac{\partial \delta}{\partial t}$ and integrating, it is predicted that $\delta = [c(m+1)vt]^{\frac{1}{m+1}}$. In spite of c=2 and m=1 in δ and we obtain $\delta = 2\sqrt{vt}$ which observes that the parameter δ can be correlated with the well settled scaling parameter for the unsteady boundary layer problems (see Schlichting[46]).

For experimental principles, the functions $f(\eta)$ and $\theta(\eta)$ grant us to define the skin friction coefficient and the Nusselt number as:

$$C_f = \frac{\mu_{f_n}}{\rho_f U^2}\left(\frac{\partial u}{\partial y}\right)_{at\, y=0} = -\frac{1}{(1-\zeta)^{2.5}}(Re x)^{-\frac{1}{2}}f''(0) \tag{26}$$

$$Nu_x = \frac{xk_{f_n}}{k_f(T_w - T_\infty)}\left(\frac{\partial T}{\partial y}\right)_{at\, y=0} = -(Re x)^{\frac{1}{2}}\frac{k_{f_n}}{k_f}\theta'(0)\left[1 + \frac{4}{3}N(C_T + \theta(0))^3\right] \tag{27}$$

Here, $Re_x = \frac{Ux}{v_f}$ is the local Reynolds number.

3. Results and Discussion

Estimation are carried out by the fourth or fifth order Range Kutta Fehlberg method with shooting technique for different values of parameters. Equations (23) and (24) developed to the boundary conditions (25) have been resolved numerically employing computer software Maple 18. If $\gamma \gg 1.0$ conforms to pure free convection, $\gamma = 1.0$ correlates to mixed convection and $\gamma \ll 1.0$ corresponds to pure forced convection. Impacts of nanoparticle shapes and solar thermal radiation energy on unsteady Hiemenz water-based Cu, Al₂O₃ and SWCNTs nanofluid flow over a porous wedge sheet are investigated for different values of parameters. In order to justify our method, we have correlated the solutions of $f(\eta), f'(\eta)$

and $f''(\eta)$ for different values of η (Table 2) with White[48] whereas $f''(0)$ *and* $\theta'(0)$ for distinct values of ζ (Table 3) with Vajravelu et al.[49] and observed them in desirable acknowledging.

Table 1: Thermophysical resources of the fluid and nanoparticles

	$\rho\ (kg/m^3)$	$cp\ (J/kgK)$	$k\ (W/mK)$	$\sigma\ (\Omega^{-1}m^{-1})$	$\beta\times10^{-5}\ (K^{-1})$
Pure water	997.1	4179	0.613	5.5	21
Copper (Cu)	8933	385	401	59.6	1.67
Al$_2$O$_3$	3970	765	40	16.7	0.85
SWCNTs	2600	42.5	6600	1.26	2.7

Table 2: Association of the present outputs with already released work

η	White [48]			Current outputs		
	$f(\eta)$	$f'(\eta)$	$f''(\eta)$	$f(\eta)$	$f'(\eta)$	$f''(\eta)$
0.0	0.00000	0.00000	0.46959	0.00000	0.000000	0.469586
0.5	0.05864	0.23423	0.46503	0.058636	0.234267	0.465028
1.0	0.23299	0.46063	0.43438	0.232986	0.460628	0.434377
2.0	0.88680	0.81669	0.25567	0.886795	0.816686	0.255665
3.0	1.79557	0.96905	0.06771	1.795567	0.969045	0.067712
4.0	2.78388	0.99777	0.00687	2.783881	0.997770	0.006870

Table 3: Correlation of the instant outputs with past broadcast work

γ	ζ	Wajravelu et al [49]		Present work	
		$f''(0)$	$\theta'(0)$	$f''(0)$	$\theta'(0)$
0	0.0	-1.001411	-2.972286	-1.0014113	-2.9722856
0	0.1	-1.175203	-2.476220	-1.1752027	-2.4762203
0	0.2	-1.218301	-2.094192	-1.2183007	-2.0941916
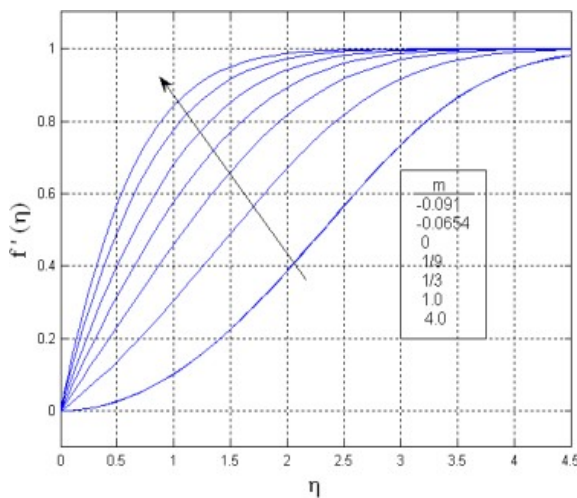
Figure 2: Effects of m on the velocity distribution in the laminar flow past a wedge

7

In the nonappearance of energy equation, in order to conform the efficiency of our numerical results, the current work is correlated with the feasible exact result in the literature. The velocity profiles for various values of m is associated with the achievable exact solution of Schlichting[46], is seen in Fig.2. It is noticed that the judgment with the theoretical result of velocity profile is desirable.

3.1 Analysis of nanoparticle volume fraction, with solar radiation energy, Figure 3:

(i)   Both $N=0.0$ and $N=1.0$, it is realized that the temperature of all the shape of the nanoparticle (sphere, cylinder and lamina) in the nanofluids (water-based Cu, Al$_2$O$_3$ and SWCNTs) increases with increase of nanoparticle volume fraction.

(ii)   In the presence of solar thermal radiation energy $N=1.0$, it is amusing to note that the mal boundary layer mal boundary layer width of lamina shape ($m=16.1576$) SWCNTs in SWCNTs-water is stronger as interacted with the other mixtures in the flow region with upturn of nanoparticle volume fraction. This recognize with the physical attitude that when the volume fraction of SWCNTs enhances the thermal conductivity and then the thermal boundary layer thickness developments.

(iii)   In general, the temperature assigning of lamina shape nanoparticles in the water-based Cu, Al$_2$O$_3$ and SWCNTs is higher than that of all the other shapes in the flow presidency in the presence of solar radiation energy.
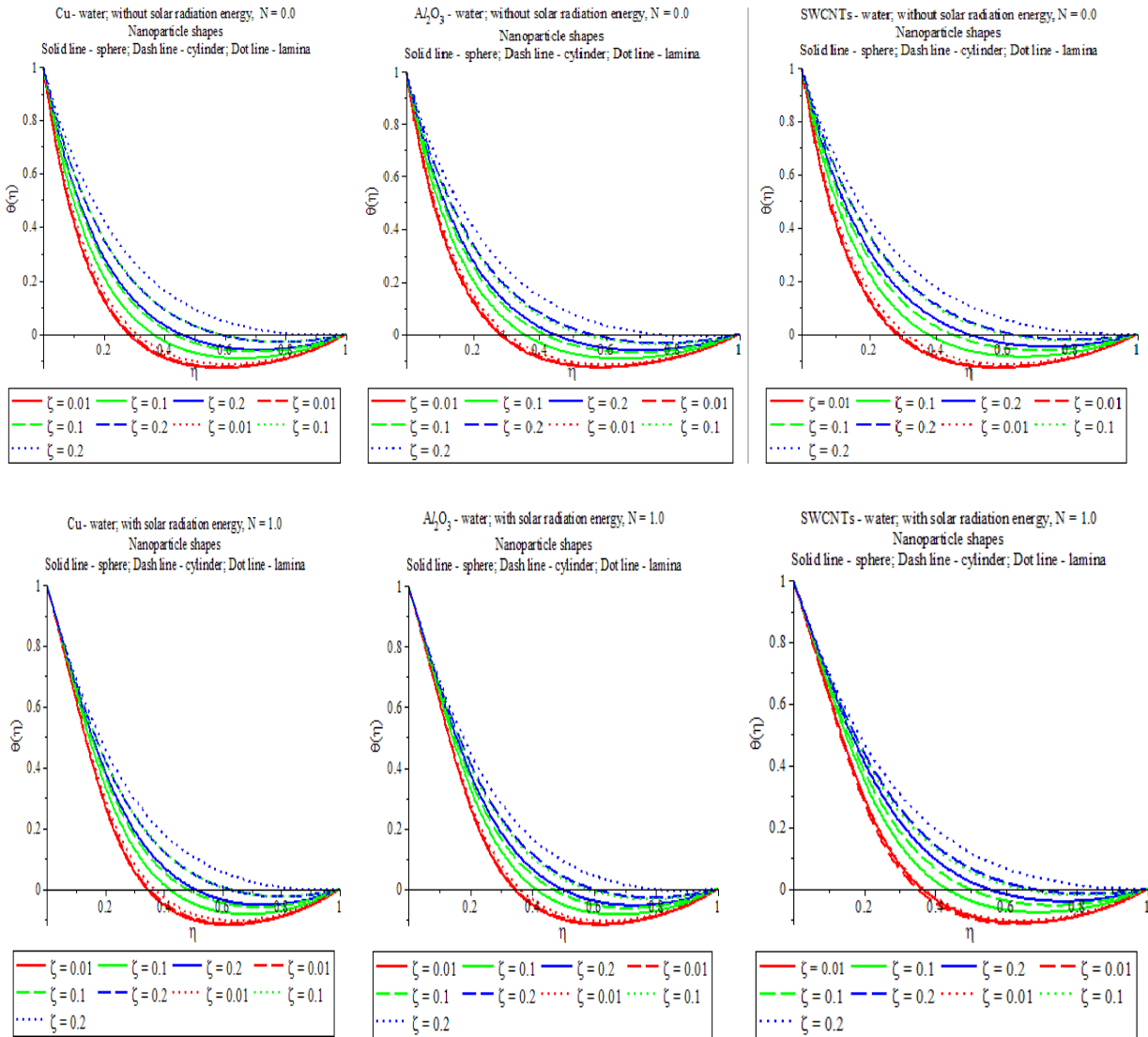
Figure 3: Nanoparticle shape and volume fraction on temperature profiles with different nanofluids with or without magnetic field.

3.2 Investigation of solar thermal radiation energy with porous strength, Figure 4:

(i) In the presence of porous medium, $\lambda=5.0$, the temperature distribution of all the shape of the nanoparticles (sphere, cylinder and lamina) in the nanofluids (water-based Cu, Al_2O_3 and SWCNTs) enhances with rise of solar thermal radiation energy.

(ii) Especially, the temperature scattering of lamina shape nanoparticles in the water-based Cu, Al_2O_3 and SWCNTs is more symbolic as compared to the other shapes in the flow tenure with increase of solar radiation energy.

(iii) The thermal boundary layer girth of lamina shape nanoparticles in the nanofluids water-based SWCNTs is more forceful as associated with the other mixtures in the flow system with boost of solar radiation energy.
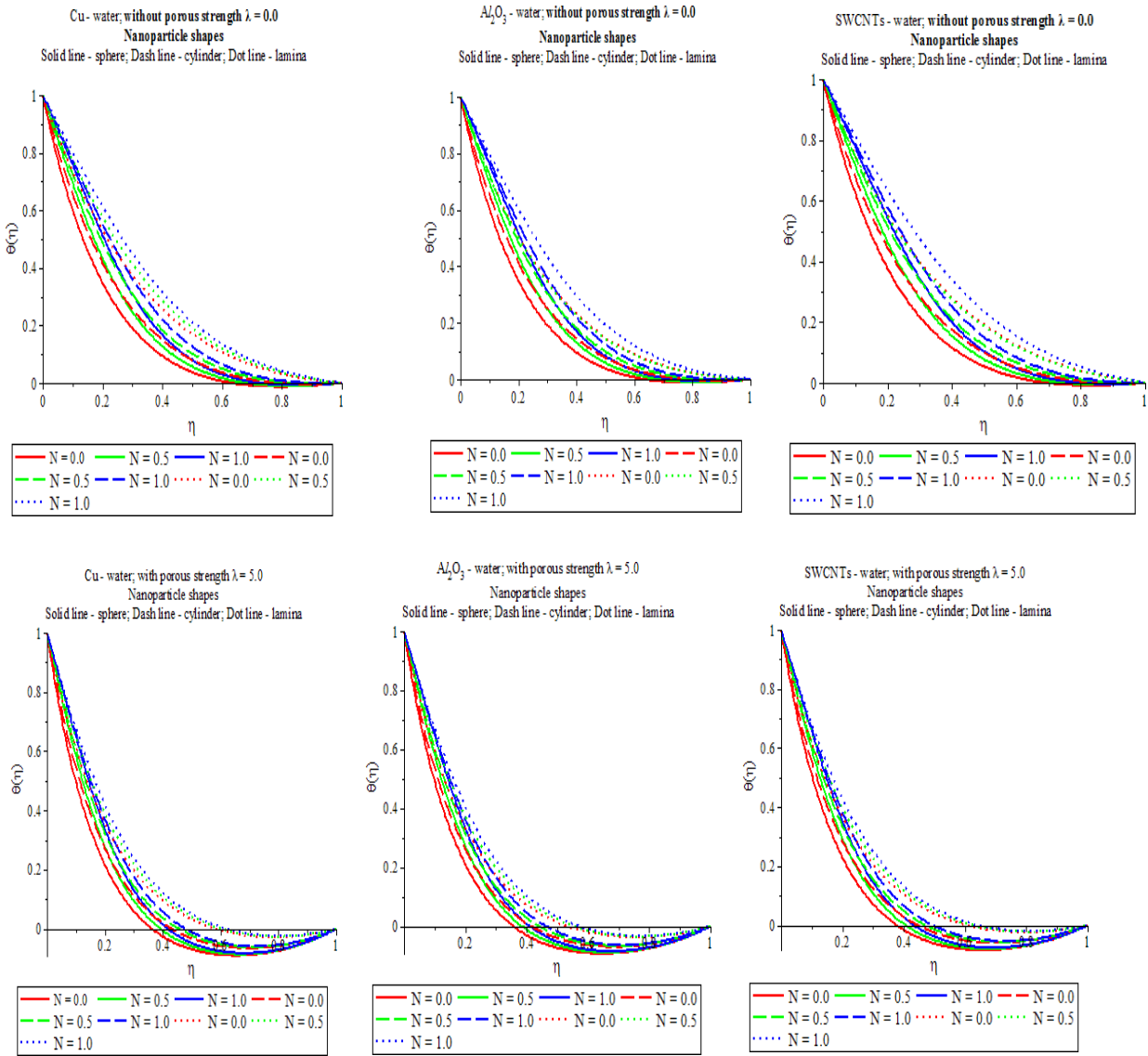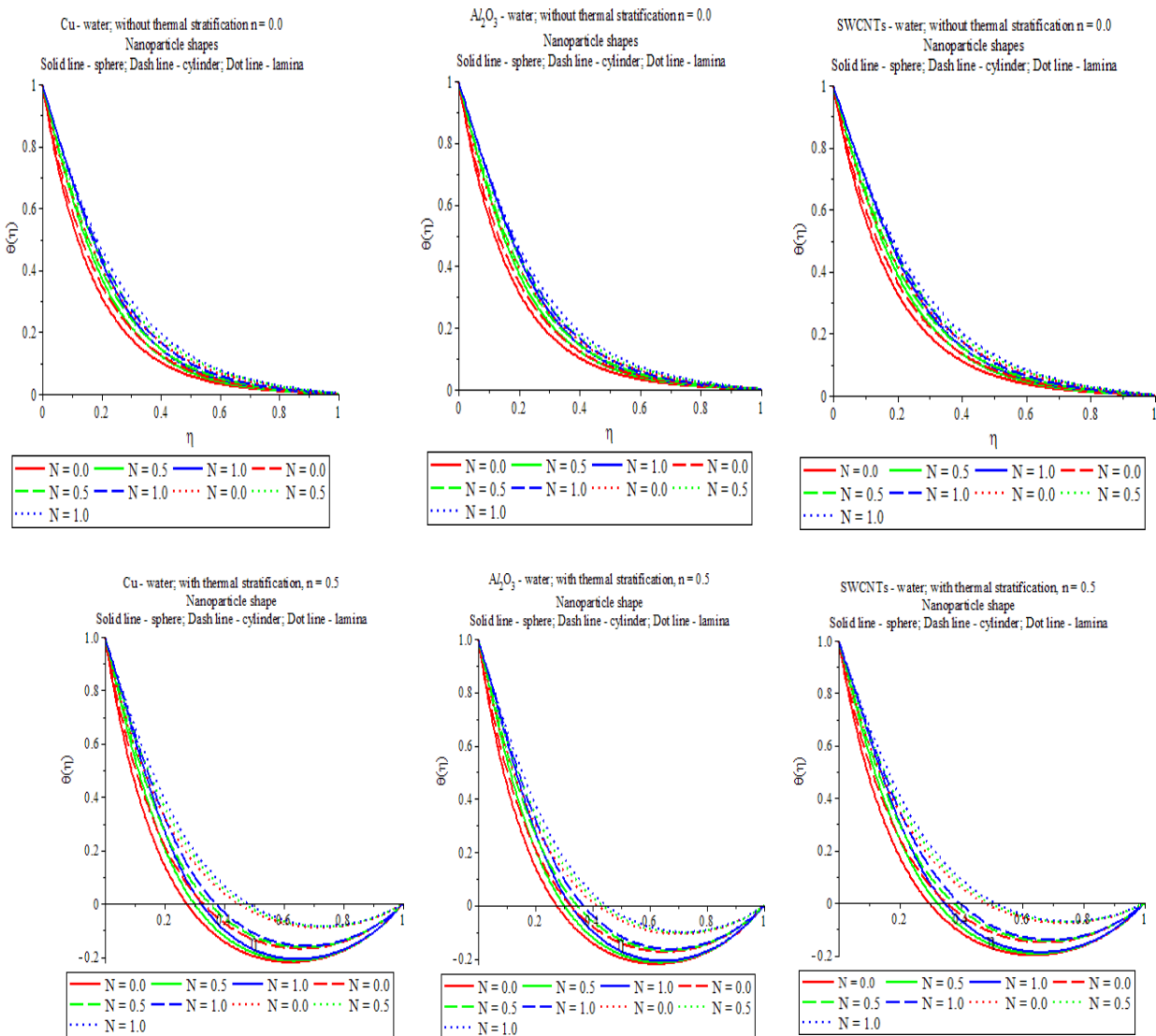

Figure 4: Nanoparticle shape and solar radiation energy on temperature profiles with different nanofluids with or without porous media

3.3 Report of solar thermal radiation energy with thermal stratification, Figure 5:

(i) In the presence of *n=0.0* (flow along the wall), it is fascinating to notice that the temperature profiles are bounded within the boundary region while the temperature assigning of nanofluids based Cu, Al₂O₃ and SWCNTs) for different shapes accelerates with growth of solar radiation energy. All the cases, negative value of the temperature profile develops in the outer boundary region. This is because of the combined effect of thermal stratification and solar thermal radiation energy.

(ii) For heat transfer characteristics mechanism, stimulating solution is the large exaggeration of the temperature field induced for $0.1 \leq n < 1$ (*n=0* refers to flow at the wall, bottom layer and *n=1* refers to flow at ambient, upper layer).

(iii) The temperature distribution of nanofluids (water-based Cu, Al₂O₃ and SWCNTs) for different shapes increases with upturn of solar radiation energy. The temperature transport of laminar shape SWCNTs in SWCNTs-water is more capable as compared to other mixtures in the flow system with upgrade of solar thermal radiation energy.

Figure 5: Nanoparticle shape and solar radiation energy on temperature profiles with different nanofluids with or without thermal stratification

3.4 Review of solar thermal radiation energy wit angle of inclination, Figure 6:

(i) Both N=0.0 and N=1.0, it is seen that the temperature of all the shape of the nanoparticles (sphere, cylinder and lamina) in the nanofluids (water-based Cu, Al$_2$O$_3$ and SWCNTs) enhances with increase of nanoparticle volume fraction. As the angle of inclination raises the impact of the buoyancy effects due to thermal diffusion reduces by an aspect of $\cos\frac{\Omega}{2}$. Therefore, the dynamic force of the fluid reduces and as a solution the temperature accelerates.

(ii) In the presence of solar thermal radiation energy N=1.0, it is amusing to note that the mal boundary layer thickness of lamina shape (m=16.1576) SWCNTs in SWCNTs-water plays a dominant role as compared with other mixture in the flow scheme with rise of angle of inclination.

(iii) The temperature distribution of lamina shape nanoparticles in the water-based Cu, Al$_2$O$_3$ and SWCNTs is more significant as compared to other mixtures in the flow regime with increase of angle of inclination. This effort of passing the absorbing nanofluid through an absorbing porous wedge medium is regarded to raise solar collection by absolute absorption in which heat falls are decreased as an output of plate temperatures.
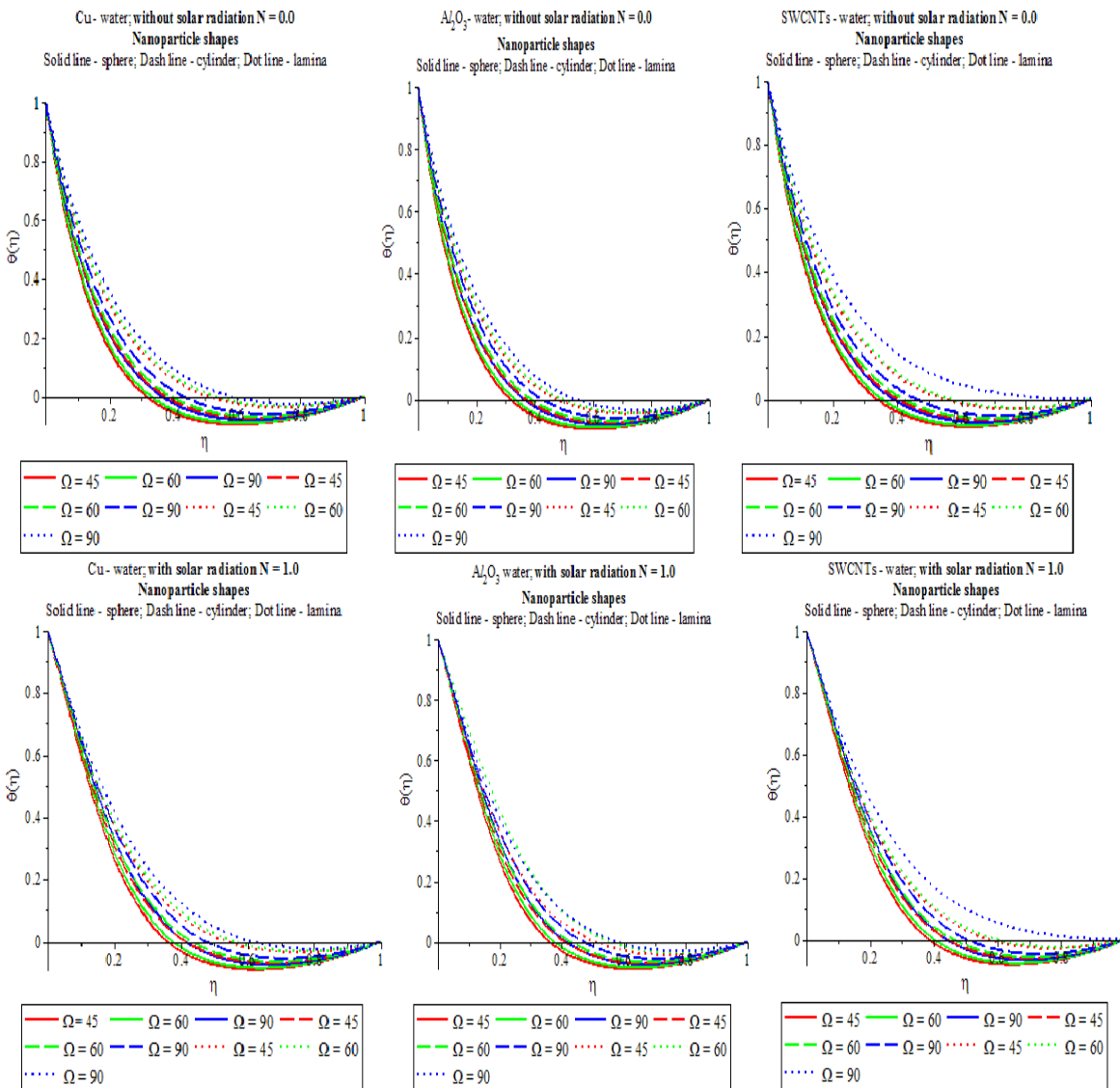

Figure 6: Nanoparticle shape and angle of inclination on temperature profiles with different nanofluids with or without solar radiation energy

3.6 Survey of rate of heat transfer, Table 4:

3.6.1 Impact of nanoparticle volume fraction without solar radiation energy

(i) The rate of heat transfer of sphere shape alumina nanoparticles in the presence of Al_2O_3 -water is stronger (ζ=0.01, $\theta'(0)$= 8.04687187) than that of all the other nanoparticle shapes in the presence of various mixtures in the flow regime.

(ii) The rate of heat transfer of lamina shape SWCNTs nanoparticles in the presence of SWCNTs-water is lower (ζ=0.2, $\theta'(0)$= 4.00008697) as compared all the other mixtures in the flow regime.

3.6.2 Performance of nanoparticle volume fraction with solar radiation energy

(i) The rate of heat transfer of sphere shape alumina nanoparticles in the presence of Al_2O_3-water is stronger (ζ=0.01; $\theta'(0)$=3.62498990) as correlated with the other mixtures in the flow regime.

(ii) The rate of heat transfer of sphere shape SWCNTs nanoparticles in the presence of SWCNTs-water is lower (ζ=0.2, $\theta'(0)$=3.27286122) as associated with the other mixtures in the flow regime which means that the SWCNTs water will be important in the cooling and heating processes.

Table 4: Nanoparticle shapes and volume fraction on rate of heat transfer with different nanofluids.

	$\theta'(0)$			
ζ	Cu - water	Al_2O_3 - water	SWCNTs - water	Shapes
0.01	8.03379135	8.04687187	8.00372625	Sphere, N=0.0 (solar radiation energy)
0.10	6.66216322	6.71737429	6.41276664	
0.20	5.68175744	6.71737429	5.30666643	
0.01	7.86248328	7.89491190	7.83159583	Cylinder, N=0.0 (solar radiation energy)
0.10	5.85968260	5.98074172	5.67126613	
0.20	4.87149884	4.97574154	4.63233094	
0.01	7.43504127	7.56300907	7.39538693	Lamina, N=0.0 (solar radiation energy)
0.10	4.83308891	5.07433223	4.71268947	
0.20	4.12329584	4.28785861	4.00008697	
0.01	3.62167437	3.62498990	3.53086381	Sphere, N=2.0 (solar radiation energy)
0.10	3.50586755	3.51584053	3.42167964	
0.20	3.42708814	3.42824839	3.27286122	
0.01	3.61574110	3.61972665	3.60804828	Cylinder, N=2.0 (solar radiation energy)
0.10	3.47858691	3.49073833	3.40663526	
0.20	3.40616504	3.40938824	3.28714266	
0.01	3.60045064	3.60792489	3.59278083	Lamina, N=2.0 (solar radiation energy)
0.10	3.44123583	3.45733730	3.38955186	
0.20	3.39022608	3.39428171	3.31747952	

4. Conclusion

Subject of nanoparticle shapes (sphere, cylinder and lamina) on Hiemenz nanofluids (water, ethylene glycol and engine oil-based Cu, Al_2O_3 and SWCNTs) flow over a porous wedge in design of solar radiation energy has been analyzed. Reorganization of heat transfer rate and temperature within the nanofluids with distinct nanoparticle shapes are predicted in terms of Figures and Tables and the issues of the analysis are placed as follows: The temperature empowering of lamina shape nanoparticles in the water-based Cu, Al_2O_3 and SWCNTs is more advanced than that of all the other shapes in the flow system with increase of solar radiation energy in the presence of all the other effects in the flow regime.

❖ The lamina shape SWCNTs in SWCNTs - water plays symbolic possessions on temperature distribution with raised of solar thermal radiation energy as compared to all the other shapes in the flow region which means that the SWCNTs water will be important in the heating processes.

❖ The rate of heat transfer of sphere shape alumina nanoparticles in the presence of Al_2O_3 - water is stronger as correlated with the other mixtures in the flow scheme.

❖ The rate of heat transfer of sphere shape SWCNTs nanoparticles in the presence of SWCNTs - water is no more significant as associated with the other mixtures in the flow regime.

It is registered that the lamina shape SWCNTs in the existence of water-based SWCNTs is researched in this work can be gainful in the solar radiation energy systems. Resultantly, the lamina shape SWCNTs in the SWCNTs-water is a more affirmation in terms of complementing the heat transfer reinforcement of the Hiemenz flow system over a porous wedge surface.

Acknowledgements

Nomenclature

| C_T	Temperature ratio	α_{f_n}	Thermal diffusivity of the nanofluid
c_p	Specific heat at constant pressure	β_f	Thermal expansion coefficient of the base fluid
g	Acceleration due to gravity	β_s	Thermal expansion coefficient of the nanoparticle
k_1	Rate of chemical reaction	ρ_f	Density of the base fluid
k^*	Absorption coefficient	ρ_s	Density of the nanoparticle
K	Permeability of the porous medium	ρ_{f_n}	Effective density of the nanofluid
k_f	Thermal conductivity of the base fluid	$(\rho c_p)_{f_n}$	Heat capacitance of the nanofluid
k_s	Thermal conductivity of the nanoparticle	σ_1	Stefan-Boltzman constant
k_{f_n}	Effective thermal conductivity of the nanofluid	κ	Thermal conductivity of the fluid
n	Thermal stratification parameter	μ_f	Dynamic viscosity of the base fluid
q''_{rad}	Incident radiation flux of intensity	μ_{f_n}	Effective dynamic viscosity of the nanofluid
T	Temperature of the fluid	δ	Time-dependent length scale
T_w	Temperature of the wall	Ω	angle of inclination of the wedge
T_∞	Temperature of the fluid far away from the wall	ξ	Dimensionless distance along the wedge
u,v	Velocity components in x and y direction	ζ	Nanoparticle volume fraction
U(x)	Flow velocity of the fluid away from the wedge		
V_0	Velocity of suction/injection		

Nanoparticle shapes
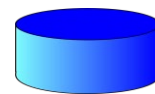
Sphere (*m*=3.0)   Cylinder (*m*=6.3698)   Lamina (*m*=16.1576)

References

1. A. Sharma, V.V. Tyagi, C.R. Chen, D. Buddhi, Review on thermal energy storage with phase change materials and applications, Renew. Sust. Energy Rev., 13 (2009), pp. 318–345.
2. A.J. Hunt, Small particle heat exchangers, Lawrence Berkeley Laboratory report no. LBL-7841, J. Renew. Sust. Energy (1978).
3. S. Choi, Enhancing thermal conductivity of fluids with nanoparticle, 66 D.A. Siginer, H.P. Wang (Eds.), Developments and Applications of Non-Newtonian Flows, ASME MD, vol. 231, FED (1995), pp. 99–105.
4. J. Buongiorno, W. Hu, Nanofluid coolants for advanced nuclear power plants, Paper no. 5705 Proceedings of ICAPP '05, Seoul (2005), pp. 15–19.
5. J. Buongiorno, Convective transport in nanofluids, ASME J. Heat Transf., 128 (2006), pp. 240–250.
6. P. Cheng, W. Minkowycz, Free convection about a vertical flat plate embedded in a porous medium with application to heat transfer from a dike, J. Geophys. Res., 82 (1977), pp. 2040–2044.
7. A. Mufuoglu, E. Bilen, Heat transfer in inclined rectangular receivers for concentrated solar radiation, Int. Commun. Heat Mass Transfer, 35 (2008), pp. 551–556.
8. R. Kandasamy, I. Muhaimin, A.B. Khamis, R.B. Roslan, Unsteady Heimenz flow of Cu-nanofluid over a porous wedge in the presence of thermal stratification due to solar energy radiation: lie group transformation, Int. J. Therm. Sci., 65 (2013), pp. 196–205.
9. K. Das, P.R. Duari, P.K. Kundu, Solar radiation effect on Cu-water nanofluid flow over a stretching sheet with surface slip and temperature jump, Arab. J. Sci. Eng., 39 (2014), pp. 9015–9023.
10. N. Anbuchezhian, K. Srinivasan, K. Chandrasekaran, R. Kandasamy, Magneto hydrodynamic effects on natural convection flow of a nanofluid in the presence of heat source due to solar energy, Meccanica, 48 (2013), pp. 307– 321.
11. T. Yousefi, F. Veysi, E. Shojaeizadeh, S. Zinadini, An experimental investigation on the effect of Al2O3–H2O nanofluid on the efficiency of flat-plate solar collectors, Renewable Energy, 39 (2012), pp. 293–298.
12. T. Yousefi, E. Shojaeizadeh, F. Veysi, S. Zinadini, An experimental investigation on the effect of pH variation of MWCNT–H2O nanofluid on the efficiency of a flat-plate solar collector, Sol. Energy, 86 (2) (2012), pp. 771–779.
13. Y. Kameya, K. Hanamura, Enhancement of solar radiation absorption using nanoparticle suspension, Sol. Energy, 85 (2) (2011), pp. 299–307.
14. A. Lenert, E.N. Wang, Optimization of nanofluid volumetric receivers for solar thermal energy conversion, Sol. Energy, 86 (1) (2012), pp. 253–265.
15. Q. He, S. Wang, S. Zeng, Z. Zheng, Experimental investigation on photothermal properties of nanofluids for direct absorption solar thermal energy systems, Energy Convers. Manage., 73 (2013), pp. 150–157.
16. T. Sokhansefat, A.B. Kasaeian, F. Kowsary, Heat transfer enhancement in parabolic trough collector tube using Al2O3/synthetic oil nanofluid, Renew. Sustain. Energy Rev., 33 (2014), pp. 636–644.
17. A.N. Al-Shamani, M.H. Yazdi, M.A. Alghoul, A.M. Abed, M.H. Ruslan, S. Mat, K. Sopian, Nanofluids for improved efficiency in cooling solar collectors – a review, Renew. Sustain. Energy Rev., 38 (2014), pp. 348–367.
18. A. Kasaeian, A.T. Eshghi, M. Sameti, A review on the applications of nanofluids in solar energy systems, Renew. Sustain. Energy Rev., 43 (2015), pp. 584–598.
19. P. Mohammad Zadeh, T. Sokhansefat, A.B. Kasaeian, F. Kowsary, A. Akbarzadeh, Hybrid optimization algorithm for thermal analysis in a solar parabolic trough collector based on nanofluid, Energy, 82 (2015), pp. 857–864.
20. M. Sardarabadi, M. Passandideh-Fard, S. Zeinali Heris, Experimental investigation of the effects of silica/water nanofluid on PV/T [Photovoltaic thermal units], Energy, 66 (2014), pp. 264–272.
21. P. Chandrasekaran, M. Cheralathan, V. Kumaresan, R. Velraj, Enhanced heat transfer characteristics of water-based copper oxide nanofluid PCM (phase change material) in a spherical capsule during solidification for energy efficient cool thermal storage system, Energy, 72 (2014), pp. 636–642.
22. A.M. Hussein, K.V. Sharma, R.A. Bakar, K. Kadirgama, A review of forced convection heat transfer enhancement and hydrodynamic characteristics of a nanofluid, Renew. Sustain. Energy Rev., 29 (2014), pp. 734–743.
23. F. Javadi, R. Saidur, M. Kamalisarvestani, Investigating performance improvement of solar collectors by using nanofluids, Renew. Sustain. Energy Rev., 28 (2013), pp. 232–245.
24. L. Syam, M.K. Sundar Singh, Convective heat transfer and friction factor correlations of nanofluid in a tube and with inserts: a review, Renew. Sustain. Energy Rev., 20 (2013), 23–35.
25. Ali. J. Chamkha, A.R.A. Khaled, Similarity solutions for hydro magnetic simultaneous heat and mass transfer, Heat Mass Transf., 37 (2001), pp. 117–125.
26. M.A. Seddeek, A.A. Darwish, M.S. Abdelmeguid, Effects of chemical reaction and variable viscosity on hydromagnetic mixed convection heat and mass transfer for Heimenz flow through porous media with radiation, Commun. Nonlinear Sci. Numer. Simul., 12 (2007), pp. 195–213.

27. R. Tsai, J.S. Huang, Heat and mass transfer for Soret and Dufour's effects on Heimenz flow through porous medium onto a stretching surface, Int. J. Heat Mass Transf., 52 (2009), pp. 2399–2406.

28. Gamal Abdel-Rahman, Thermal-diffusion and MHD for Soret and Dufour's effects on Heimenz flow and mass transfer of fluid flow through porous medium onto a stretching surface, Physica B, 405 (2010), pp. 2560–2569.

29. K. Hiemenz, Die Grenzschicht an einem in den gleichfoÈrmigen FluÈssigkeitsstrom eingetauchten geraden Kreiszylinder, Dingl. Poltech. J., 326 (1911), pp. 321–410.

30. K.A. YihThe effect of uniform suction/blowing on heat transfer of Magnetohydrodynamic Hiemenz flow through porous media, Acta Mech., 130 (1998), pp. 147–158.

31. N.G. Kafoussias, N.D. Nanousis, Magnetohydrodynamic laminar boundary layer flow over a wedge with suction or injection, Can. J. Phys., 75 (1997), pp. 733–781.

32. Anjali Devi, R. Kandasamy, Effects of heat and mass transfer on MHD laminar boundary layer flow over a wedge with suction or injection, J. Energy Heat Mass Transf., 23 (2001), pp. 167–178.

33. T. Watanabe, Thermal boundary layer over a wedge with uniform suction or injection in forced flow, Acta Mech., 83 (1990), pp. 119–126.

34. M.A. Hossian, Viscous and Joule heating effects on MHD free convection flow with variable plate temperature, Int. J. Heat Mass Transf., 35 (1992), pp. 3485–3492.

35. Kuo Bor-Lih, Heat transfer analysis for the Falkner–Skan wedge flow by the differential transformation method, Int. J. Heat Mass Transf., 48 (2005), pp. 5036–5042.

36. W.T. Cheng, H.T. Lin, Non-similarity solution and correlation of transient heat transfer in laminar boundary layer flow over a wedge, Int. J. Eng. Sci., 40 (2002), pp. 531–540.

37. A.A. Avramenko, S.G. Kobzar, I.V. Shevchuk, A.V. Kuznetsov, L.T. Iwanisov, Symmetry of turbulent boundary layer flows: investigation of different Eddy viscosity models, Acta Mech., 151 (2001), pp. 1–14.

38. E.V. Timofeeva, J.L. Routbort, D. Singh, Particle shape effects on thermophysical properties of alumina nanofluids, Journal of Applied Physics, 106 (1) (2009) 014304.

39. S.U.S. Choi SUS (2009) Nanofluids: from vision to reality through research, J Heat Transf., 131(2009) 1–9.

40. E.M. Sparrow, R.D. Cess, Radiation heat transfer, Hemisphere, Washington, 1978.

41. A. Raptis, Radiation and free convection flow through a porous medium, Int. Comm. Heat Mass Transfer, 25 (1998) 289-295.

42. M.Q. Brewster, Thermal Radiative Transfer Properties, John Wiley & Sons, New York, 1972.

43. M.A. Sattar, Unsteady hydromagnetic free convection flow with Hall current, mass transfer and variable suction through a porous medium near an infinite vertical porous plate with constant heat flux, International Journal of Energy Research, 18 (1994) 771–77.

44. S.M. Aminossadati, B. Ghasemi, Natural convection cooling of a localized heat source at the bottom of a nanofluid-filled enclosure, Eur. J. Mech. B/Fluids, 28 (2009) 630–640.

45. J.C.A. Maxwell, A Treatise on Electricity and Magnetism, 2 unabridged 3rd Ed., Clarendon Press, Oxford, UK, 1891.

46. H. Schlichting, Boundary Layer Theory, McGraw Hill Inc., New York, 1979.

47. P.V.S.N., Murthy, S. Mukherjee, D. Srinivasacharya, P.V.S.S.S.R., Krishna, Combined radiation and mixed convection from a vertical wall with suction / injection in a non-Darcy porous medium, Acta Mechanica, 168 (2004), 145-156.

48. F.M. White, Viscous Fluid Flows, third edition. McGraw-Hill, New York, 2006.

49. K. Vajravelu, K.V. Prasad, Jinho Lee, Changhoon Lee, I. Pop, A. Robert, Van Gorder, Convective heat transfer in the flow of viscous Ag-Water and Cu-water nanofluids over a stretching surface, International Journal of Thermal Sciences, 50 (2011), 843-851.

50. N.G. Kafoussias, N.D. Nanousis, Magnetohydrodynamic laminar boundary layer flow over a wedge with suction or injection, Canadian Journal of Physic, 75 (1997) 733-781.